MRS Advances (2022) 7:1022–1027
https://doi.org/10.1557/s43580-022-00371-7

ORIGINAL PAPER

Charpy impact toughness in all directions with respect to the rolling direction of API 5L X52 pipeline steel

G. Terán[1] · S. Capula-Colindres[1] · F. Chávez[2] · J. C. Velázquez[3] · E. Torres-Santillan[3] · D. Angeles-Herrera[4] · O. Goiz[5]

Received: 23 August 2022 / Accepted: 28 October 2022 / Published online: 8 November 2022

Abstract

In this study, the Charpy V-notch (CVN) values were investigated in all directions [longitudinal-transverse (L-T), T-L, short-transverse (S-T), T-S, L-S, S-L, and at 45°] with respect to the rolling direction (RD) of American Petroleum Institute (API) 5L X52 steel welded by electric resistance welding (ERW). In addition, the microstructures and fracture surfaces were examined by scanning electron microscopy (SEM). The Charpy specimens were machined according to ASTM E23 and tested at room temperature. The experimental results showed that the CVN values depended on the direction of the RD. Additionally, a fracture surface analysis performed with SEM showed fibrous fracture, dimples, and secondary cracks. Microstructures of ferrite and perlite were obtained, which are typical of X52 steel.

Introduction

The American Petroleum Institute (API) [1] determines the standard for the manufacture of two levels of product specification (PSL1 and PSL2) of seamless and welded steel pipes used in transportation systems in the oil and natural gas industry. API 5L steel pipes are widely used for gas, hydrocarbon, and crude oil transportation in the oil industry, which are generally designed for a minimum life of 20 years [2]. In the oil and gas industry, there are some methods to manufacture pipelines by seam-welding [3–5]. Electric resistance-welded (ERW), longitudinal-seam submerged arc-welded (LSAW), and spiral submerged arc-welded (SSAW) pipes are employed to fabricate seam-welded pipelines. Seam-welded lines can be produced through a continuous process from a rolled strip of a plate. A forming process, such as the U-forming-O-forming Expansion (UOE) or the J-forming-C-forming-O-forming (JCO) process, is usually employed [4–6]. During the pipeline manufacturing process, anisotropy is an important characteristic. Anisotropy affects the material properties, strength, and toughness [5]. In addition, anisotropy affects material properties as a function of the rolling direction (RD) [7]. The Charpy test measures material properties such as the ductility or toughness [8]. Toughness may be anisotropic, and the Charpy impact test is one method to measure impact toughness [9]. Some studies have determined pipeline toughness and anisotropy by testing Charpy specimens in different directions with respect to the RD, obtaining excellent results [10–14]. However, only some Charpy V-notch (CVN) values have been obtained.

In this study, the CVN impact test was employed to measure the fracture toughness of an API 5L X52 ERW pipe. The CVN specimens were extracted in different orientations with respect to the RD. Based on the RD, longitudinal-transverse (L-T), T-L, short-transverse (S-T), T-S, L-S, S-L, and 45° directions were considered. The CVN samples were tested according to ASTM E23 [15].

✉ S. Capula-Colindres
selenecapula@gmail.com

G. Terán
gerardoteranm@gmail.com

1 Departamento de Metalurgia, CECYT 2-IPN, CDMX, 11200 Mexico City, Mexico

2 Departamento de Metalurgia y Materiales, ESIQIE-IPN, CDMX, 07738 Mexico City, Mexico

3 Departamento de Ingeniería Química Industrial, ESIQIE-IPN, CDMX, 07738 Mexico City, Mexico

4 TecNM/ITS de Tantoyuca (ITSTa), Subdirección de Posgrado e Investigación, Desv. Lindero Tametate s/n, Col. La Morita, Tantoyuca, 92100 Veracruz, Mexico

5 Departamento de Biociencias e Ingeniería, CIIEMAD-IPN, CDMX, 07340 Mexico City, Mexico

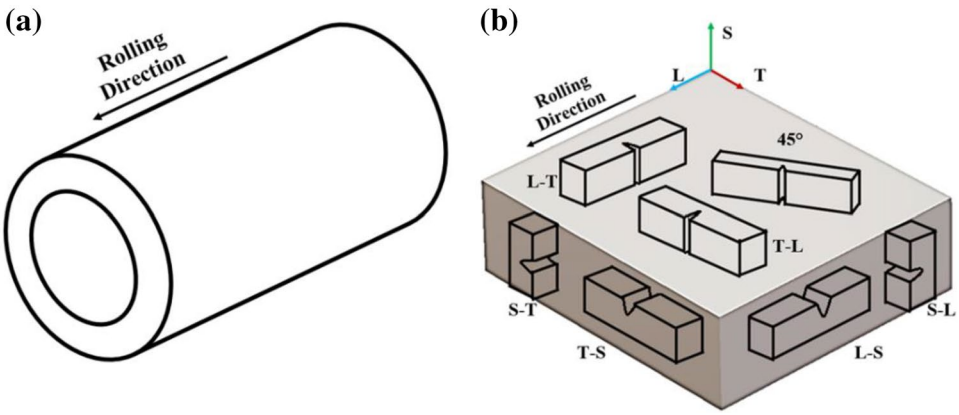

Fig. 1 **a** Diagram of American Petroleum Institute (API) 5L X52 electric resistance-welded (ERW) pipe showing the rolling direction, and **b** extracted Charpy specimens in the rolling direction, longitudinal-transverse direction (L–T), and short-transverse direction (S-T)

Experimental work

CVN impact test

The wall thickness and diameter of the API 5 L X52 ERW pipe were, respectively, 25.4 mm and 406.4 mm. This type of pipe (X52 ERW) is considered PSL 2 and has been removed from service. Figure 1a, b shows schematics of the pipeline and RD and extracted CVN specimens, respectively. CVN specimens were prepared in orientations such as L-T, T-L, S-T, T-S, L-S, S-L, and at 45° with respect to the RD. One Charpy specimen was tested for each orientation condition. These specimens were prepared according to the ASTM E23 standard [15] using a Charpy model 74 tester with a capacity of 0.0–274 ft-lb. Charpy standard specimens with dimensions of $10 \times 10 \times 55$ mm were employed with respect to the RD. The tests were conducted at room temperature. The specimens were cut in the T-S, L-S, and L-T orientations for microstructure observations. After mechanical grinding and polishing, the metallographic specimens were etched with a 3% Nital solution and observed by scanning electron microscopy (SEM).

To achieve a length of 55 mm for the Charpy specimens in the S-T and S-L orientations, extension-welding was necessary, and an X52 plate was employed. The tungsten inert gas (TIG) process was selected. To obtain the microstructure, the transverse direction (2-Plane T-S), longitudinal direction (3-Plane L-S), and upper direction (1-Plane L-T) were evaluated.

Results and discussion

CVN values

Table 1 lists the CVN values, and Fig. 2 graphically presents these data. The CVN values for all conditions were similar

Table 1 Charpy V-notch (CVN) values for an X52 pipeline

Specimens	Joules
L-T (longitudinal-transverse)	206.10
T-L	211.82
45°	185.50
S-T (short-transverse)	229.71
T-S	210.85
L-S	209.76
S-L	182.49

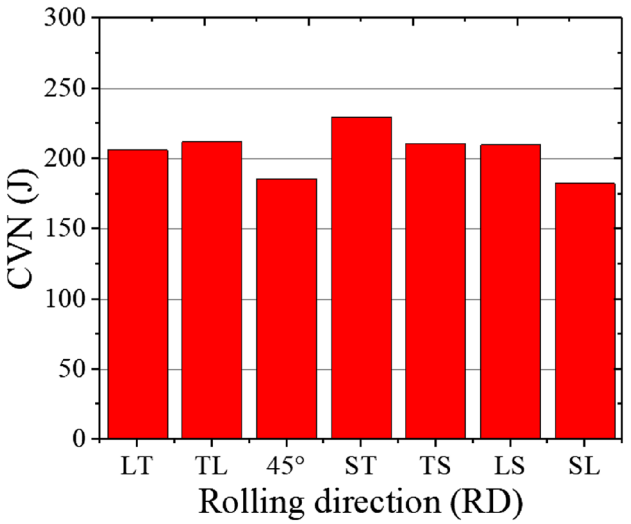

Fig. 2 Charpy V-notch (CVN) values with respect to the rolling direction

to each other. A comparison of the angle variation (T-L, 45°, and L-T conditions) with respect to the RD was performed, and the CVN values were higher for the T-L condition, followed by L-T, and finally, the 45° condition. The Charpy energy values of the X52 pipe were compared with respect to the RD, and these values decreased in the order of S-T, T-L, T-S, L-S, L-T, 45°, and S-L. Different studies have

reported Charpy values in different directions with respect to the RD in pipelines, showing serious anisotropy depending on the notch direction [4, 10–14]. Anisotropy is an important issue in the mechanical behavior of API 5L pipelines. [12, 16]. Anisotropy can arise from several factors, such as chemical segregation, variation in the shape and size of grains, non-metallic inclusions, and crystallographic texture [4]. Such stringer-shaped inclusions are known to cause anisotropy in mechanical properties such as tensile ductility and fracture toughness [3, 6]. The mechanical properties of API 5L pipelines depend on their microstructural characteristics [17, 18].

Microstructures obtained

Figure 3 shows micrographs of the ERW pipe in the T-S, L-S, and L-T planes. As shown in this figure, the ERW pipe had uniform grains in all directions because the grains were distributed along the RD during the manufacturing process. The grain size of the welded pipeline was 9.5–10 µm. The microstructures shown in Fig. 3a, c corresponded to general ferrite (white) and pearlite (black) structures, respectively, and the microstructures shown in Fig. 3b of the welded pipeline consisted of ferrite and pearlite strongly elongated in the RD. During plastic deformation in cold or hot work, grains are elongated in the direction of the applied stress. Therefore, the ferrite grain size varies along different directions, resulting in anisotropic mechanical properties [19]. The pearlite and ferrite grains were usually oriented in the direction of lamination. This behavior is known as banding. In the 45° direction, a combination of microstructures was observed in the longitudinal and transverse directions. Banding is more visible in the laminate direction than in the transverse direction [20]. Grain size and shape variations in different directions can also cause anisotropy [19].

Fracture surfaces of the Charpy specimens

Figure 4 shows all the Charpy specimens fractured under all conditions. As shown in this figure, the Charpy surfaces exhibited substantial plastic deformation. All the specimens had ductile behavior. This result occurred because the experiments were performed at room temperature, and API 5 L X52 steel has this toughness behavior under these conditions. Fractography of the specimens revealed a dimpled surface with fibrous fracture [9]. Macroscopically, plastic deformation associated with fracture was detected for all the surfaces with a shiny, fibrous appearance, indicating a combination of ductile and brittle fracture mechanisms [21, 22]. In addition, shear lips were presented owing to high shear stresses in combination with abrupt changes in the stress state toward the end of the fracture stage. Microscopically, a combination of ductile fracture with nucleation growth and coalescence of microvoids was observed, which absorbed relatively large amounts of energy [23]. Figure 5 shows the fractography of several different Charpy

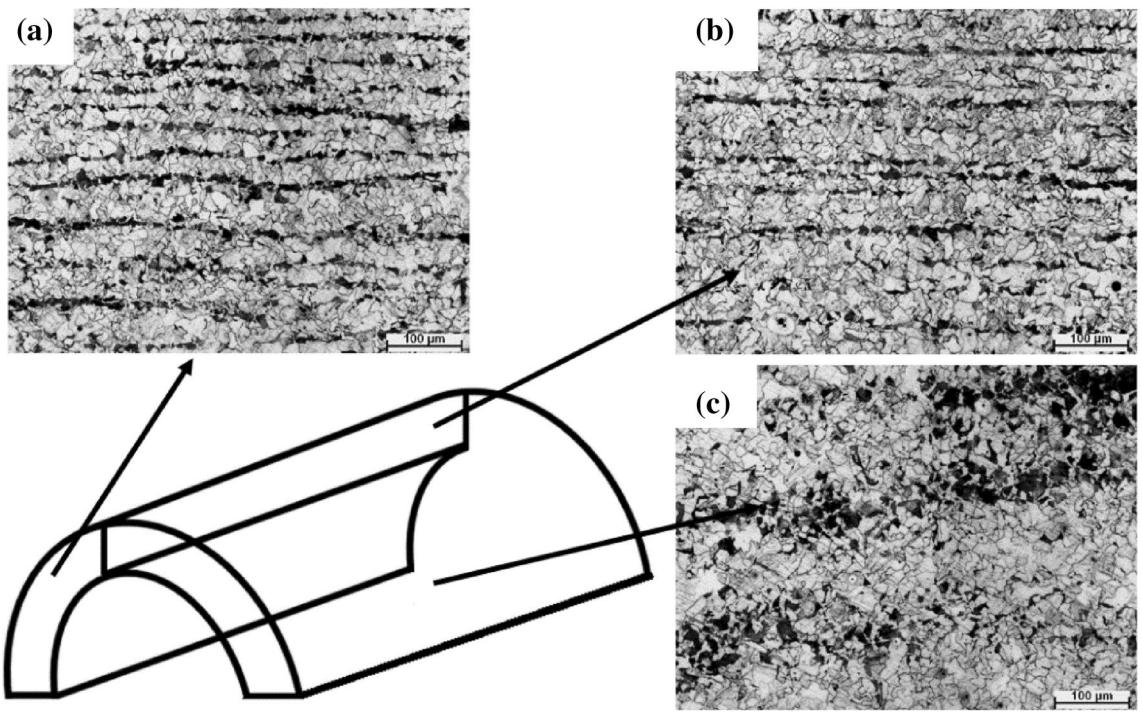

Fig. 3 Microstructures for all conditions, **a** transverse short (T-S), **b** longitudinal short (L-S), and **c** L-T

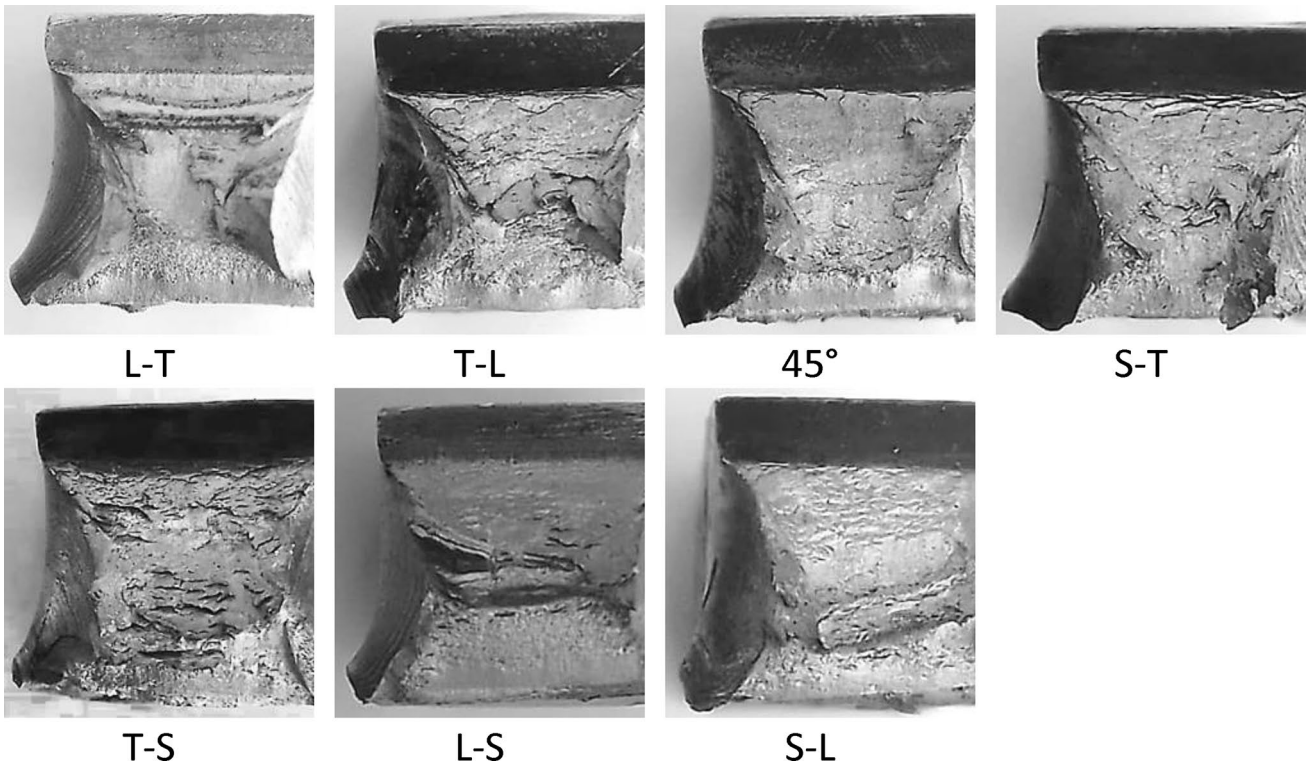

Fig. 4 Fracture surfaces of the Charpy specimens for all conditions (Abbreviations: L, longitudinal; T, transverse; and S, short)

specimens. These ductile fractures exhibited ductile dimples nucleated by inclusions or precipitates [24] (Fig. 5a). Ductile fractures have a dimpled surface owing to the tearing of the material and plastic deformation. In the case of ductile fracture, secondary cracks indicate crack deflection with more energy absorption, resulting in better toughness (see Fig. 5b, c). The coalescence of voids results in the development of a shear lip, which is responsible for a higher upper-shelf energy fracture [9]. These holes have a parabolic profile. On the same surface, there are cleaved areas corresponding to fragile areas. The height and sharpness of the shear lips are directly proportional to the fracture toughness and ductility of the material.

Defects are present in the microstructures of steels used for the manufacture of pipes, such as delamination or non-metallic inclusions [25, 26]. In most cases, non-metallic inclusions have a negative effect on the mechanical properties [27].

In the manufacturing of pipelines, delamination can occur in ferrite and pearlite microstructures with pearlite bands. For example, Teran et al. [20] reported delamination in the transverse direction of a pipeline. Delamination occurs in the planes parallel to the surface of the RD. Delamination is also observed in the S-T and T-S conditions. All the defects present in steel used for the manufacture of pipelines compromise the integrity of the steel pipeline, which can cause catastrophic failure. Similarly, these defects reduce the ability of the pipe to operate under safe conditions. In addition, the mechanical properties deteriorate.

Conclusion

The Charpy impact test was employed to obtain the CVN values in an API 5L X52 ERW steel in the L-T, T-L, S-T, T-S, L-S, S-L, and 45° directions with respect to the RD. The CVN values of the L-T, T-L, 45°, S-T, T-S, L-S, and S-L directions were 206, 211, 185, 229, 210, 209, and 182 J, respectively. The CVN values decreased in the order of S-T, T-L, T-S, L-S, L-T, 45°, and S-L. The microstructures obtained in API 5 L X52 steel were ferritic and pearlitic, elongated in the RD, causing anisotropy. In addition, the grain size was 9.5–10 μm. The fracture surface exhibited substantial plastic deformation, resulting in high toughness. In addition, the fracture surface had fibrous fractures, dimples, cracks, and secondary cracks. With these defects, the mechanical properties of steel decreases and can compromise the structural integrity of pipelines. The present work presents all the CVN values with respect to the RD in the API 5L X52 steel.

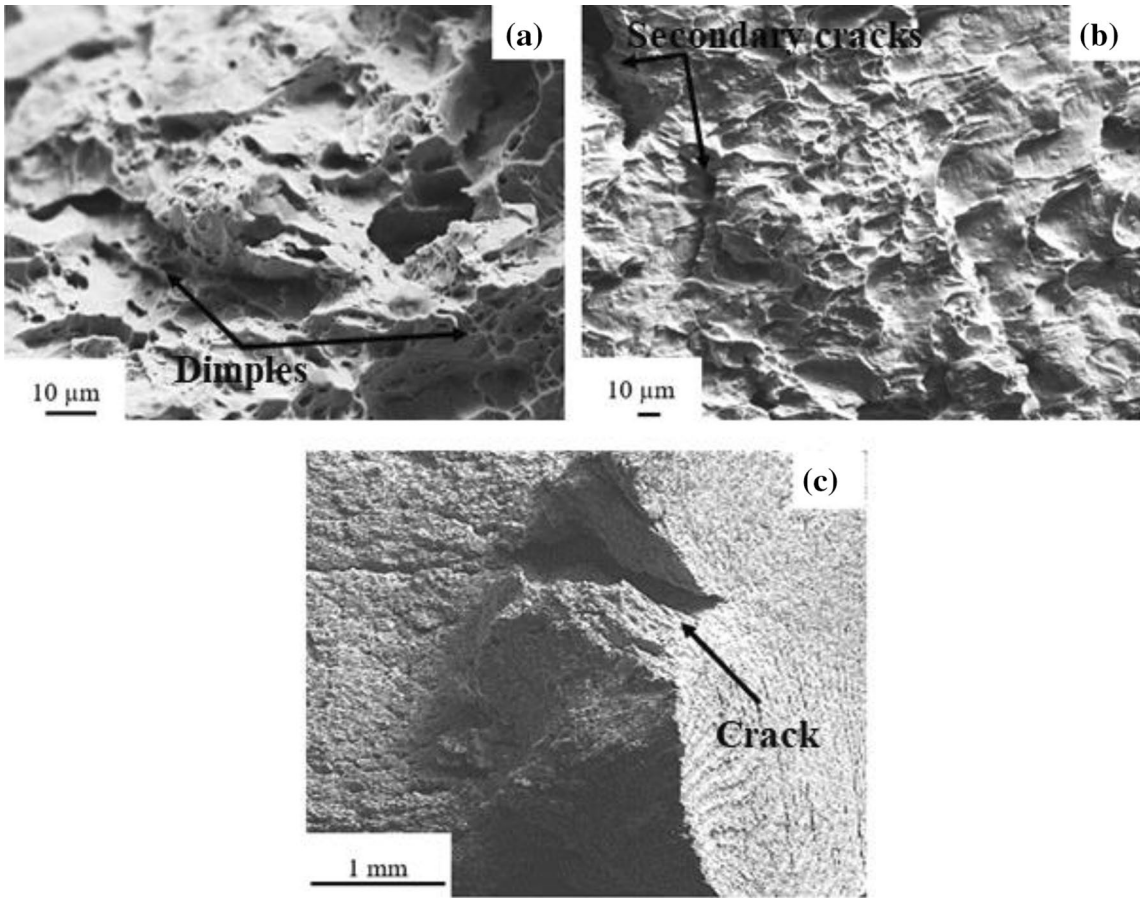

Fig. 5 Fracture surface morphology showing ductile behavior, **a** dimples, **b** secondary cracks, and **c** a crack

Acknowledgments The authors thank the Instituto Politécnico Nacional (IPN) and CONACYT for the facilities used in this research.

Declarations

Conflict of interest The authors declare no conflict of interest regarding the preparation of this article. All co-authors have seen and agreed with the contents of the manuscript, and there are no financial interests to report. We certify that the submission is an original work and is not under review by any other publication.

Data availability The datasets generated and/or analyzed during the current study are available from the corresponding author upon reasonable request.

References

1. ANSI/API Specification for Line Pipe (2010).
2. http://catarina.udlap.mx/u_dl_a/tales/documentos/mgd/gomez_f_ja/apendiceB.pdf. Accessed 1 April, 2022
3. M.W. Braestrup, J.B. Andersen, L.W. Andersen, M. Bryndum, C.J. Christensen, N.J.R. Nielsen, *Design and Installation of Marine Pipelines* (Blackwell Science Ltd, Hoboken, 2005)
4. D. Alkazraji, *A Quick Guide to Pipeline Engineering* (Woodhead Publishing Limited, Cambridge England, 2008)
5. R.R. Winston, *Oil and Gas Pipeline Integrity and Safety Handbook* (Wiley, New York, 2015)
6. S. Kyriakides, E. Corona, *Mechanics of Offshore Pipelines Buckling and Collapse* (Elsevier, New York, 2007)
7. A. Ghosh, P. Modak, R. Dutta, D. Chakrabarti, Mater. Sci. Eng. A **654**, 298–308 (2016)
8. T.C. Park, B.S. Kim, J.H. Son, Y.K. Yeo, Korean J. Met. Mater. **59**(1), 61–66 (2021)
9. A. Waqas, X. Qin, J. Xiong, C. Zheng, H. Wang, Metals **9**(11), 1–12 (2019)
10. X.L. Yang, Y.B. Xu, X.D. Tan, D. Wu, Mater. Sci. Eng. A **641**, 96–106 (2015)
11. J. Jang-Bog, L. Jung-Suk, J. Jae-Il, Mater. Lett. **61**(29), 5178–5180 (2007)
12. O.L. Garcia, R. Petrov, J.H. Bae, L.A.I. Kestens, K.B. Kang, Adv. Mater. Res. **15–17**, 840–843 (2007)
13. M.S. Joo, D.W. Suh, J.H. Bae, H.K.D.H. Bhadeshia, Mater. Sci. Eng. A **546**, 314–322 (2012)
14. X.L. Yang, Y.B. Xu, X.D. Tan, D. Wu, Mater. Sci. Eng. A **607**, 53–62 (2014)
15. ASTM E23-18. Standard Test Methods for Notched Bar Impact Testing of Metallic Materials (2018).
16. J.B. Ju, J.S. Lee, J. Jang, Mater. Lett. **61**(29), 5178–5180 (2007)
17. W. Wang, Y. Shan, K. Yang, Mater. Sci. Eng. A **502**(1–2), 38–44 (2009)

18. ASTM E1268-19, Standard Practice for Assessing the Degree of Banding or Orientation of Microstructures (2019).
19. E. Anelli, D. Colleluori, J.C. Gonzalez, G. Cumino, H. Quintana, M. Tivelli, *Sour service X65 seamless linepipe for offshore special applications*. ISOPE-I-13-377 (2001).
20. J. Teran-Guillen, Evaluación de la tenacidad a la fractura en la dirección corta de tubería de conducción de hidrocarburos, (Ph.D. thesis), Instituto Politécnico Nacional (2007)
21. C. Zong, G. Zhu, W. Mao, Mater. Sci. Eng. A **563**, 1–7 (2013)
22. M.P. Manahan Jr., C.N. McCowan, M.P. Manahan, J. ASTM Int. **5** (7) (2008).
23. ASTM A370-09. Standard Test Methods and Definitions for Mechanical Testing of Steel Products (2009).
24. P. Fassina, F. Bolzoni, G. Fumagalli, L. Lazzari, L. Vergani, A. Sciuccati, Eng. Fract. Mech. **81**, 43–45 (2012)
25. D. Angeles-Herrera, A. Albiter-Hernández, R. Cuamatzi-Melén-dez, A.J. Morales-Ramírez, J. Test. Eval. **45**(2), 687–694 (2017)
26. D. Angeles-Herrera, A. Albiter, R. Cuamatzi-Meléndez, G. Terán, G. Ochoa-Ruiz, J. Test. Eval. **46**(5), 2110–2120 (2018)
27. H. Tervo, A. Kaijalainen, T. Pikkarainen, S. Mehtonen, D. Porter, Mater. Sci. Eng. A **697**, 184–193 (2017)